Published in final edited form as:
Arch Ophthalmol. 2012 October ; 130(10): 1291–1300. doi:10.1001/archophthalmol.2012.2270.

Evaluation of normal human foveal development using optical coherence tomography and histologic examination

Adam M. Dubis, PhD[1,a], **Deborah M. Costakos, MD, MSc**[2], **C. Devika Subramaniam, MD**[2], **Pooja Godara, MD**[2], **William J. Wirostko, MD**[2], **Joseph Carroll, PhD**[1,2,3], and **Jan M. Provis, PhD**[4]

[1]Department of Cell Biology, Neurobiology, & Anatomy, Medical College of Wisconsin, Milwaukee, WI 53226

[2]Department of Ophthalmology, Medical College of Wisconsin, Milwaukee, WI 53226

[3]Department of Biophysics, Medical College of Wisconsin, Milwaukee, WI 53226

[4]ARC Centre of Excellence in Vision Science, JCSMR & ANU Medical School, Australian National University, Canberra, ACT, Australia 0200

Abstract

Objective—Assess outer retinal layer maturation during late gestation and early postnatal life using optical coherence tomography (OCT) and histology.

Methods—Thirty-nine subjects ranging from 32 weeks post-menstrual age (PMA) to 4 years were imaged using a hand held OCT (102 imaging sessions). Foveal images from 16 subjects (21 imaging sessions) were normal and evaluated for inner retinal excavation and presence of outer retinal reflective bands. Reflectivity profiles of central, parafoveal, and perifoveal retina were extracted and compared to age-matched histological sections.

Results—Foveal pit morphology in infants was generally distinguishable from adults. Reflectivity profiles showed a single hyper-reflective band at the fovea in all infants less than 42 weeks PMA. Multiple bands were distinguishable in the outer retina at the perifovea by 32 weeks PMA, and at the fovea by 3 months post term. By 17 months postnatal the characteristic appearance of four hyper-reflective bands was evident across the foveal region. These features are consistent with previous results from histology. A ‘temporal divot’ was present in some infants and foveal pit morphology and extent of inner retinal excavation was variable.

Conclusions—Hand-held OCT imaging is a viable technique for evaluating neonatal retinas. In premature infants, who do not develop ROP, the foveal region appears to follow a developmental time course similar to *in utero* maturation.

Clinical Relevance—As pediatric OCT imaging becomes more common, a better understanding of normal foveal and macular development is needed. Longitudinal imaging offers the opportunity to track postnatal foveal development in preterm infants where poor visual outcomes are anticipated or to track treatment outcomes in this population.

Introduction

The fovea centralis is a feature of all anthropoid primate retinas. The foveal avascular zone (FAZ), increased cone density, and excavation of inner retinal neurons characterize the

[a]Corresponding author: Adam M. Dubis, Medical College of Wisconsin, The Eye Institute, 925 North 87th Street, Milwaukee, WI 53226, Tel.: +1-414-955-2051, Fax: +1-414-955-6690, adubis@mcw.edu.

foveal region. The most salient feature of the human fovea is the shallow pit that is left behind by the lateral displacement of the inner retinal layers (*fovea* is Latin for "pit"). Before and during foveal formation, cones become tightly packed, elongate, and migrate centripetally.[1–3] The processes of cone packing and pit development in humans have been examined in a number of histological studies.[1–7] While the site of the future fovea can be identified as early as 12 weeks PMA using both morphological criteria[3, 8] and molecular cues,[7, 9–12] the pit itself does not emerge until after the FAZ is defined at around 24–26 weeks PMA. Later gestational changes include centrifugal migration of inner retinal neurons, resulting in progressive reduction of the ganglion and bipolar cell layers at the fovea. During the last trimester, photoreceptors are relatively immature at the foveal center, compared with parafoveal and perifoveal locations.[13] During this period the retinal pigment epithelium (RPE) also develops interdigitations with the immature outer segments.[1, 2, 7] Postnatally, the foveal pit contour continues to be modified by cellular migration, reaching maturity at roughly 18 months post term.[2] Photoreceptor elongation and displacement into the fovea also continues postnatally, and reports indicate that foveal cone density reaches the lower range reported for adults by 4 years of age.[1, 2] The exact relationship between foveal pit development and photoreceptor mosaic maturation remains unclear.[3, 14, 15]

Optical coherence tomography (OCT) enables visualization of retinal lamina and the organization of the outer retina.[16,17, 18] Previously, OCT imaging had been limited to cooperative and fixating subjects. However, the recent availability of handheld systems enables imaging of pediatric populations, with clinical applications including shaken baby syndrome[19, 20] and retinopathy of prematurity (ROP).[21–24] Recent work from one group has aimed to increase the efficiency of pediatric OCT imaging, providing some insights into development.[25,26] Advances in OCT image acquisition[27, 28] with reinvestigation by anatomists,[17, 29] has raised questions about the initial anatomical assignment of layers observed with OCT.[16, 18, 26, 27] Defining the correlation between OCT bands and photoreceptor structure is important for understanding foveal development.

Using handheld OCT, we examined postnatal features of foveal development in a series of pediatric subjects.[1, 2, 7, 8, 24, 26] Across subjects of different ages, we compared emerging retinal layers in OCT with age-matched histological sections. We used these comparisons and information available in the literature to define reflectance bands in pediatric OCT images.[17, 18] We also examined the variability in foveal morphology in this pediatric population. A better understanding of what is visualized by OCT will enable reliable interpretation *in vivo* developmental data, and facilitate the identification of normal versus pathologic features in a clinical setting.

Methods

Subjects

Research on human subjects followed the tenets of the Declaration of Helsinki and was approved by Institutional Review Boards at the Medical College of Wisconsin and Children's Hospital of Wisconsin. Informed consent was obtained from parents of all minor subjects after explanation of the nature and possible consequences of the study. One adult subject provided his own consent. Thirty-nine pediatric subjects (26 males, 13 females) ages 30 weeks PMA and older were recruited from local communities surrounding the Medical College of Wisconsin. Thirty-five were from the NICU at Children's Hospital of Wisconsin, and four subjects presented at the Medical College of Wisconsin Eye Institute for an exam under anesthesia (EUA). For imaging, eyes were dilated and accommodation suspended using Cyclomydril (Alcon, Inc., Fort Worth, TX, USA). Artificial tears were used in all subjects (Saline drops or Systain Ultra; Alcon, Inc., Fort Worth, TX, USA). For the infants, a lid speculum was used to keep the eye open during imaging. Imaging was performed after

clinical evaluation in all cases. To be considered 'normal', at no time could subjects develop cystoid macular edema (CME), and could not have ROP worse than stage 2, consistent with previously used criteria.[26] A pediatric ophthalmologist (DMC) assessed progression of ROP and presence of CME on OCT images was determined by consensus of four graders.

HHP-SDOCT Imaging

OCT imaging was performed using the Bioptigen Hand Held Probe SD-OCT (HHP-SDOCT) (Bioptigen, Research Triangle Park, NC, USA). Reference arm position and instrument focus were initially set based on information provided by Maldonado *et al*,[25] with additional adjustments done if required to improve image quality. The nominal scan size for all subjects was 8×8 mm, with a scan density of 1000 A-scans/100 B-scans (except DC_0368, nominal scan size 6×6 mm cube). The setting assumes an axial length of 24 mm, though given the shorter axial length of our population, the actual scan length is less (~6 mm). Individual variation in axial length would further alter the scan length for each subject. This provides a slightly different lateral resolution for each subject, however this scan size was selected to cover the maximum amount of retinal area (allowing visualization of the macula and edge of the optic nerve in a single scan). Images were exported in AVI format using on-instrument software, and frames containing the macula were extracted.

Histological Sections

Histological images were selected from a database of images assembled from sections of human and macaque retinas collected by Jan Provis and Anita Hendrickson. Montages were assembled from high-resolution images taken using a Zeiss HP digital camera, through a Zeiss 25x objective lens at final optical magnification of 312.5x, between 1995 and 2012 at the University of Washington, Seattle, or The Australian National University, Canberra. Sections were montages by JP using Adobe Photoshop CS5. Macaque tissue was paraffin-embedded, while all human samples were embedded in methacrylate and both samples were stained with Richardson's Stain.

Age and layer matching histological section and OCT images

OCT images were age-matched with three histological images of human retinas at 35 weeks PMA, 41 weeks PMA, and 13 years post term. Because of the rarity of human donor retinas aged between 25 and 40 weeks PMA, we selected images from macaque retina at fetal day (Fd) 131 as approximately equivalent to the human retina at 32 weeks PMA. To establish a valid comparative time point we used the caecal period (CP) - the period between conception and eye opening - as a 'unit' of development. The CP is 196 days long in humans, compared with 123 days in macaques. Initial formation of the fovea is dependent on definition of the FAZ, which occurs at around 85% CP in macaques, but slightly later in humans at ~ 90% CP (Table 1). Thirty-two weeks PMA in humans (224 days post-conception) is 44 days after definition of the FAZ (Table 1), which is equivalent to 22% of the human CP. Twenty-two (22) percent of the CP in macaques is 27 days; 27 days after definition of the macaque FAZ is 133 days post conception. The Fd131 retina is the closest approximation to 32 weeks PMA in the human available in our dataset. OCT data from a 35 weeks PMA infant was compared to 35 weeks PMA human histological sample. OCT data from a 40 weeks PMA infant was compared to a 41 week PMA histological section. Finally, OCT images from an adult (28 years old) and a 17-month-old pediatric subject were compared to sections from the 13-year-old donor.

For comparisons of OCT and histological sections, we assigned five bands (0 to 4) to the outer retinal layers. Bands 1–4 were assigned based on the recent work of Spaide and Curcio,[29] with an additional 'band 0' at the interface between the outer plexiform layer (OPL) and outer nuclear layer (ONL) which includes the photoreceptor pedicles and

synapses. Band 1 was assigned to the external limiting membrane (ELM). Band 2 was assigned to the inner segment ellipsoid (ISe).[30,30] Bands 3 and 4 are comprised of the photoreceptor/RPE microvilli interface and RPE/Bruch's membrane, respectively.

Qualitative Analysis

The lateral scale for OCT and histology images was adjusted to facilitate comparisons at specific locations. Histological images were calibrated from the original corresponding grid images, while OCT images were corrected based on age-specific axial length estimates previously reported.[25] Longitudinal reflectivity profiles (LRP) were generated from OCT images using ImageJ.[31] To increase signal-to-noise ratios, and facilitate band assignment, gray scale reflectivity values from five consecutive lateral positions were averaged to construct each LRP. LRPs were analyzed for the presence or absence of each of five outer retinal bands in the foveola (central 0.5 mm, ~1.5 visual angle), parafovea (0.5–1 mm eccentricity, ~3° Nasal) and perifovea (2mm eccentricity, ~6° Nasal). Congruency in band assignment between the OCT, LRP and histology is shown in Figure 1.

Results

Subjects Imaged

As summarized in Supplemental Table 1, we obtained clinically useable images in 72% of exams in awake infants in the NICU (71/98) and 100% (4 of 4) of exams imaged as part of an EUA. We defined "clinically useable" as a volume image in which the foveal center and both slopes were visible with sufficient image quality for the graders to determine the presence or absence of CME. These numbers are comparable to other reports.[23, 26] The 75 clinically useable images were acquired from 33 subjects. Since the current study was designed to assess normal foveal development, subjects deemed abnormal (> Stage 2 ROP, intervention for ROP or presence of CME) were excluded from subsequent analysis. Five were removed because they developed stage 3 ROP or required intervention for ROP, while 12 were removed because they developed CME. The remaining 16 subjects were considered normal for the purposes of this study (15 male, 1 female). The 21 exams from these subjects are shown in Figure 2, with multiple images obtained on three subjects (DC_0499-2 images, DC_0576-3 images, and DC_0688-3 images).

Photoreceptor and Foveal Pit Maturation

As expected from histological data, the foveal pit was present in images obtained from the youngest subject, a 32 weeks PMA infant.[2, 26] Over the series of subjects imaged, we observed variability in foveal morphology even among age-matched subjects (Figure 2). For example, the foveas of the 3 youngest subjects (32 weeks PMA, Figure 2, top row) have different appearances; subject DC_0572 has a deeper depression than the other 32 weeks PMA infants, as well as the 33 weeks PMA infants in the second row. In this series, the foveal pit continues to deepen and widen through 43 weeks PMA, but is still immature at this point, having a distinct inner nuclear layer lining the floor of the pit. The subject at 52 weeks PMA (DC_0593) is the youngest to show complete excavation of all inner retinal layers.

In all subjects younger than 43 weeks PMA, only 2 hyper-reflective bands were detected in the fovea. However, multiple hyper-reflective bands were detected in the perifoveal region in even the youngest subjects. In contrast to previous reports,[26] we found the outer retina to be adult-like, in terms of the appearance of hyper-reflective bands, at 17 months postnatal.

Macaque Fd131 to Human 32 weeks PMA

In the 32 weeks PMA OCT image there is a distinct band, which we refer to as 'band 0', across the fovea (Figure 3). After examining a range of specimens we conclude that band 0 reflects the layer of cone pedicles. A thicker hyper-reflective band is present at the level of the RPE and RPE/photoreceptor interactions, which we refer to as band 3/4. This is consistent with the appearance of the histological image, which shows that the foveal photoreceptor nuclei are only a single layer deep, but have short axons that separate the cone pedicles from the layer of nuclei. The foveal photoreceptors have short inner and outer segments that are barely distinguishable from the RPE. In the parafovea, the OCT image shows an increase in the separation between these two hyper-reflective bands, indicative of increased elongation of photoreceptor cells in the parafovea compared to the foveola. This is consistent with the features seen in the Fd131 histological section, which shows that parafoveal cones have smaller soma diameters and longer axons when compared with foveal cones (Figure 3C1 & 3C2). This difference would account for the increased separation between the hyper-reflective bands in the parafovea. In the perifovea, there is a broadening of the outermost band in the OCT image, seen as a double peak in the LRP profile (Figure 3C1). Comparison with the histological image at this location indicates that, in addition to being more elongated than at the fovea, the photoreceptors in the perifovea have better developed inner and outer segments. Elongation of the outer segments results in increased separation of the ELM from the RPE and accounts for the appearance of an additional band (band 1/2) in the perifoveal OCT image.

A feature of the OCT image from DC_0368 (32 weeks PMA) and DC_0499 (32 weeks PMA) but not DC_0572 (32 weeks PMA) is the presence of an upward inflection in band 0 in the foveola. Such differences illustrate that the enormous variability in foveal anatomy seen in adults, likely has its origins early in development.

Comparison of Human Histology and OCT images at 35 weeks PMA

The image of the 35 weeks PMA subject (Figure 4B) shows increased excavation of the central fovea, which still includes all of the retinal layers. This interpretation is consistent with the features of the 35 weeks PMA histological section (Figure 4A). The OCT image shows only two hyper-reflective bands in the fovea (0 and 3/4), consistent with histology images showing foveal photoreceptors lacking well-formed outer segments resulting in opposition of the ELM to the RPE (Figure 4C3). Although the histology shows that photoreceptors in the parafovea have somewhat more elongated cell bodies and rudimentary inner/outer segments, there is little increase in the distance between the ELM and RPE; consistent with the parafoveal OCT image showing only 2 hyper-reflective bands (Figure 4C2). However, the perifoveal OCT image shows an additional band in the nasal outer retina (Figure 4C1). At a comparable location in the histological section, photoreceptor inner and outer segments are more elongated than in the fovea (Figure 4C3) resulting in better separation of the ELM from the RPE. This is consistent with the presence of an additional hyper-reflective band in the OCT image, just emerging in the LRP, which most likely corresponds to band 1/2.[29] Closer to the disc, separation of bands 1/2 from 3/4 is more distinct. This is consistent with more advanced development of photoreceptors close to the disc at this age.

Comparison of Human Histology and OCT images at 40 weeks PMA

Both the OCT and the histological images show foveas with all of the retinal layers (Figure 5A,5B). Although the histological section shows a broader, flatter fovea than the OCT (probably due to individual variation), both images show a layer of cone pedicles (band 0 on the OCT) at approximately 50% depth of the fovea (Figure 5C3). In the parafovea, the histology shows the cell bodies of photoreceptors are more tightly packed than at the fovea;

distinct inner segments and rudimentary outer segments are present, such that the ELM and RPE are separated by only a few microns (Figure 5C2). The OCT image at the parafovea is similar to the fovea, in that only 2 hyper-reflective bands are present – band 0, and band 3/4. In the perifovea, however, the photoreceptor inner segments are more prominent than at the fovea or parafovea, and the outer segments are better developed; these two changes result in a separation of the ELM and RPE of approximately 42μm at this location (Figure 5C1). Consistent with this advancing maturation, the OCT shows 4 distinct bands in the perifovea, which appear to correspond to the cone pedicles (band 0), the ELM (band 1), ISe (band 2) and the RPE/outer segment associations (band 3/4).

The maturation sequence of foveal, parafoveal (1 mm eccentricity) and perifoveal (2 mm eccentricity) photoreceptors is shown in Figure 6, to which notional hyper-reflectivity bands have been assigned. The sequence shows that the layer of cone pedicles is distinct at each location from about 30 weeks PMA onwards, and its position in the retinal profile makes this the most likely source of hyper-reflective band 0. The foveal sequence (top row) suggests that the ELM only begins to distinctly separate from the RPE in the postnatal period, and that separation of bands 1–4 is unlikely to be observed until maturation of the foveal cones is nearly complete. In developing retinas, separation of the features associated with the hyper-reflective bands is better in the perifovea than parafovea, and both are better than at the fovea. In the adult retina separation of bands 1–4 is most distinct in the fovea.

Comment

Foveal maturation and photoreceptor elongation can be studied *in vivo* with SD-OCT imaging in young infants, including those of premature age. Our imaging success rate of 72% in the NICU is comparable to previous reports for similar populations,[26] although lower than reported by Vinekar *et al*, who reported 100% success in 79 eyes using a different imaging system.[23, 32] Although the effects of CME and retinal schisis were not directly addressed in this study, they were present in a significant percentage of the population (39%), which differs from previous reports.[23,25] Uncooperative neonates and an unsupported imaging arm provided challenges not encountered in adult imaging. Our methods differed somewhat from those of Maldonado *et al*.;[25, 26] we used a lid speculum and scleral depressor and chose to use a standard image size and offline lateral correction based on age rather than change image size.

This report provides further *in vivo* evidence that foveal development proceeds *ex utero*, consistent with other reports.[25] Additionally, we observed variation in foveal pit morphology in age-matched subjects in our population. Two examples of this variation are seen in the 32/33 weeks PMA infants. In the three samples from the 32 weeks PMA infants, there is variability in photoreceptor layer thickness (distance from peak 0 to peaks 3/4, which comprises the ONL and photoreceptor IS and OS, if present). In two subjects photoreceptor layer thickness decreases closer to the fovea, consistent with histological reports.[9, 13, 14] However in two subjects at this age there was a prominent upwards tilt in band 0 at the fovea, suggesting elongation of the central most cones. Another difference was the 33 weeks PMA infants had shallower foveal depressions than the 32 weeks PMA infants. Subject DC_0604 had residual ganglion cell layer at the fovea, while other 32/33 weeks PMA subjects did not. These developmental differences indicate that the enormous variability seen in adults originates during the earliest stages of foveal development.[33, 34]

We also observed irregularities in the curvature of the retina in our sample population. Several eyes showed a sharp bend and an abrupt upward inflexion of the retina, temporal to the parafovea in subjects between 30 and 40 weeks; we refer to this as a ‘temporal divot’ (*i.e.* DC_0572, DC_0604, DC_0688 in Figure 2). The bend appears to be at the temporal

edge of the 'dome' in the GC layer, formed by migrations of the GC;[8] the upward inflexion of the retina may reflect the contour of the sclera of a small eye. Irregularities in the contour of the developing eye are common in histological preparations, commonly attributed 'histological artifact' due to retinal shrinkage and mechanical distortion. However, the presence of irregularities *in vivo* suggests a physiological explanation; one possibility is that developmentally, retinal growth is not perfectly matched to scleral growth. The relationship of the retina to the sclera during the late stages of development could be addressed through longitudinal OCT studies.

Previous histological reports suggest that the fovea continues to mature for several years after birth.[2] Our data suggest that morphological development of the fovea may be complete by around 17 months, at least in some individuals. Maldonado *et al.* suggested that the retina is not fully mature at 15 months in that the subject imaged lacked separation of bands 3/4, although the image was not shown.[26] It is possible that in the two-month window from 15 to 17 months the photoreceptors undergo rapid elongation, making band 3 (RPE/photoreceptor interaction) separate from band 4. Alternatively, better image quality may reveal separation of bands 3 and 4 in our neonate. Nonetheless, our findings, and those of Maldonado *et al.*[25] indicate that elongation of central photoreceptors in human retina takes place on a more abbreviated timescale than previously reported,[1] and may be complete as early as 18 months of age. Further exploration of normal *ex utero* development will facilitate the identification of anatomical aberrations in a clinical setting.

Supplementary Material

Refer to Web version on PubMed Central for supplementary material.

Acknowledgments

J. Carroll is the recipient of a Career Development Award from Research to Prevent Blindness. This study was supported by NIH Grants P30EY001931, T32EY014537, R01EY017607, The E. Matilda Ziegler Foundation for the Blind, Thomas M. Aaberg, Sr., Retina Research Fund, RD and Linda Peters Foundation, and an unrestricted departmental grant from Research to Prevent Blindness. Funding for J. Provis was from Australian Research Council Centres of Excellence Program Grant (CE0561903). Part of this investigation (done at MCW) was conducted in a facility constructed with support from Research Facilities Improvement Program Grant Number C06 RR-RR016511 from the National Center for Research Resources, National Institutes of Health. The authors thank the donors of human fetal eyes for research, Anita Hendrickson for sharing with JP her collection of human and macaque retinal sections. The authors would also like to thank C. Brault, D. Felzer, S.O. Hansen and P.M. Summerfelt for technical assistance.

References

1. Yuodelis C, Hendrickson A. A qualitative and quantitative analysis of the human fovea during development. Vision Research. 1986; 26(6):847–855. [PubMed: 3750868]
2. Hendrickson AE, Yuodelis C. The morphological development of the human fovea. Ophthalmology. 1984; 91(6):603–612. [PubMed: 6462623]
3. Diaz-Araya C, Provis JM. Evidence of photoreceptor migration during early foveal development: a quantitative analysis of human fetal retinae. Visual Neuroscience. 1992; 8(6):505–514. [PubMed: 1586652]
4. Mann, I. The Development of the Human Retina. New York: Grune & Stratton; 1950.
5. Yamada E. Some structural features of the fovea centralis in the human retina. Archives of Ophthalmology. 1969; 82:151–159. [PubMed: 4183671]
6. Bach L, Seefelder R. Entwicklungsgeschichte des menschlichen auges. 1914
7. Abramov I, Gordon J, Hendrickson A, Hainline L, Dobson V, LaBossiere E. The retina of the newborn human infant. Science. 1982; 217:265–267. [PubMed: 6178160]

8. Provis JM, Diaz CM, Dreher B. Ontogeny of the primate fovea: a central issue in retinal development. Progress in Neurobiology. 1998; 54:549–581. [PubMed: 9550191]
9. Cornish EE, Madigan MC, Natoli R, Hales A, Hendrickson AE, Provis JM. Gradients of cone differentiation and FGF expression during development of the foveal depression in macaque retina. Visual Neuroscience. 2005; 22(4):447–459. [PubMed: 16212702]
10. Kozulin P, Natoli R, Bumsted O'Brien KM, Madigan MC, Provis JM. Differential expression of anti-angiogenic factors and guidance genes in the developing macula. Molecular Vision. 2009; 15:49–59.
11. Kozulin P, Natoli R, Bumsted O'Brien KM, Madigan MC, Provis J. The cellular expression of antiangiogenic factors in fetal Primate macula. Investigative Ophthalmology & Visual Science. 2010; 51(8):4298–4306. [PubMed: 20357200]
12. Kozulin P, Natoli RCMM, Bumsted O'Brien KM, Provis JM. Gradients of Eph-A6 expression in primate retina suggest roles in both vascular and axon guidance. Molecular Vision. 2009; 15:2649–2662. [PubMed: 20011078]
13. Springer AD, Troilo D, Possin D, Hendrickson AE. Foveal cone density shows a rapid postnatal maturation in the marmoset monkey. Visual Neuroscience. 2011; 28:473–484. [PubMed: 22192504]
14. Springer AD, Hendrickson AE. Development of the primate area of high acuity. 3: Temporal relationships between pit formation, retinal elongation and cone packing. Visual Neuroscience. 2005; 22(2):171–185. [PubMed: 15935110]
15. Provis JM, Penfold PL, Cornish EE, Sandercoe TM, Madigan MC. Anatomy and development of the macula: specialisation and the volunerability to macular degeneration. Clinical and Experimental Optometry. 2005; 88(5):269–281. [PubMed: 16255686]
16. Huang D, Swanson EA, Lin CP, et al. Optical coherence tomography. Science. 1991; 254(5035): 1178–1181. [PubMed: 1957169]
17. Curcio CA, Messinger JD, Sloan KR, Mitra A, McGwin G, Spaide RF. Human chorioretinal layer thicknesses measured in macula-wide, high-resolution histologic sections. Investigative Ophthalmology & Visual Science. 2011; 52(7):3943–3954. [PubMed: 21421869]
18. Drexler W, Fujimoto J. State-of-the-art retinal optical coherence tomography. Progress in Retinal and Eye Research. 2007; 27:45–88. [PubMed: 18036865]
19. Scott AW, Farsiu S, Enyedi LB, Wallace DK, Toth CA. Imaging the infant retina with a hand-held spectral-domain optical coherence tomography device. American Journal of Ophthalmology. 2009; 147(2):364–373. e362. [PubMed: 18848317]
20. Koozekanani DD, Weinberg DV, Dubis A, Beringer J, Carroll J. Hemorrhagic retinoschisis in shaken baby syndrome with spectral domain optical coherence tomography. Ophthalmic Surgery, Lasers, & Imaging. 2010; 41:e1–e3.
21. Chavala SH, Farsiu S, Maldonado R, Wallace DK, Freedman SF, Toth CA. Insights into advanced retinopathy of prematurity using handheld spectral domain optical coherence tomography imaging. Ophthalmology. 2009; 116:2448–2456. [PubMed: 19766317]
22. Maldonado RS, Chavala SH, Farsiu S, Wallace DK, Freedman SF, Toth CA. Insights into advanced retinopathy of prematurity utilizing hand-held spectral domain optical coherence tomography (SDOCT) imaging. Investigative Ophthalmology and Visual Science. 2009; 50 E-Abstract 5728.
23. Vinekar A, Avadhani K, Sivakumar M, et al. Understanding clinically undetected macular changes in early retinopathy of prematurity on spectral domain optical coherence tomography. Investigative Ophthalmology & Visual Science. 2011; 52(8):5183–5188. [PubMed: 21551410]
24. Cabrera MT, Maldonado RS, Toth CA, et al. Subfoveal fluid in healthy full-term newborns observed by handheld spectral-domain optical coherence tomography. Am J Ophthalmol. Jan; 2012 153(1):167–175. e163. [PubMed: 21925640]
25. Maldonado RS, Izatt JA, Sarin N, et al. Optimizing hand-held spectral domain optical coherence tomography imaging for neonates, infants and children. Investigative Ophthalmology & Visual Science. 2010; 51(5):2678–2685. [PubMed: 20071674]
26. Maldonado RS, O'Connell RV, Sarin N, et al. Dynamics of human foveal development after premature birth. Ophthalmology. 2011; 118(12):2315–2325. [PubMed: 21940051]

27. Drexler W, Morgner U, Kartner FX, et al. In vivo ultrahigh-resolution optical coherence tomography. Optics Letters. 1999; 24(17):1221–1223. [PubMed: 18073990]

28. Drexler W. Ultrahigh-resolution optical coherence tomography. Journal of Biomedical Optics. Jan-Feb;2004 9(1):47–74. [PubMed: 14715057]

29. Spaide RF, Curcio CA. Anatomical correlates to the bands seen in the outer retina by optical coherence tomography: literature review and model. Retina. 2011; 31(8):1609–1619. [PubMed: 21844839]

30. Hood DC, Zhang X, Ramachandran R, et al. The inner segment/outer segment border seen on optical coherence tomography is less intense in patients with diminished cone function. Investigative Ophthalmology & Visual Science. 2011; 52(13):9703–9709. [PubMed: 22110066]

31. Abramoff MD, Magelhaes PJ, Ram SJ. Image processing with ImageJ. Biophotonics International. 2004; 11(7):36–42.

32. Vinekar A, Sivakumar M, Shetty R, et al. A novel technique using spectral-domain optical coherence tomography (Spectralis, SD-OCT + HRA) to image supine non-anaesthetized infants: utility demonstrated in aggresive posterior retinopathy of prematurity. Eye. 2010; 2010:1–4.

33. Wagner-Schuman M, Dubis AM, Nordgren RN, et al. Race- and sex-related differences in retinal thickness and foveal pit morphology. Investigative Ophthalmology & Visual Science. 2010; 52:625–634. [PubMed: 20861480]

34. Dubis AM, Hansen BR, Cooper RF, Beringer J, Dubra A, Carroll J. The Relationship Between the Foveal Avascular Zone and Foveal Pit Morphology. Investigative Ophthalmology & Visual Science. 2012

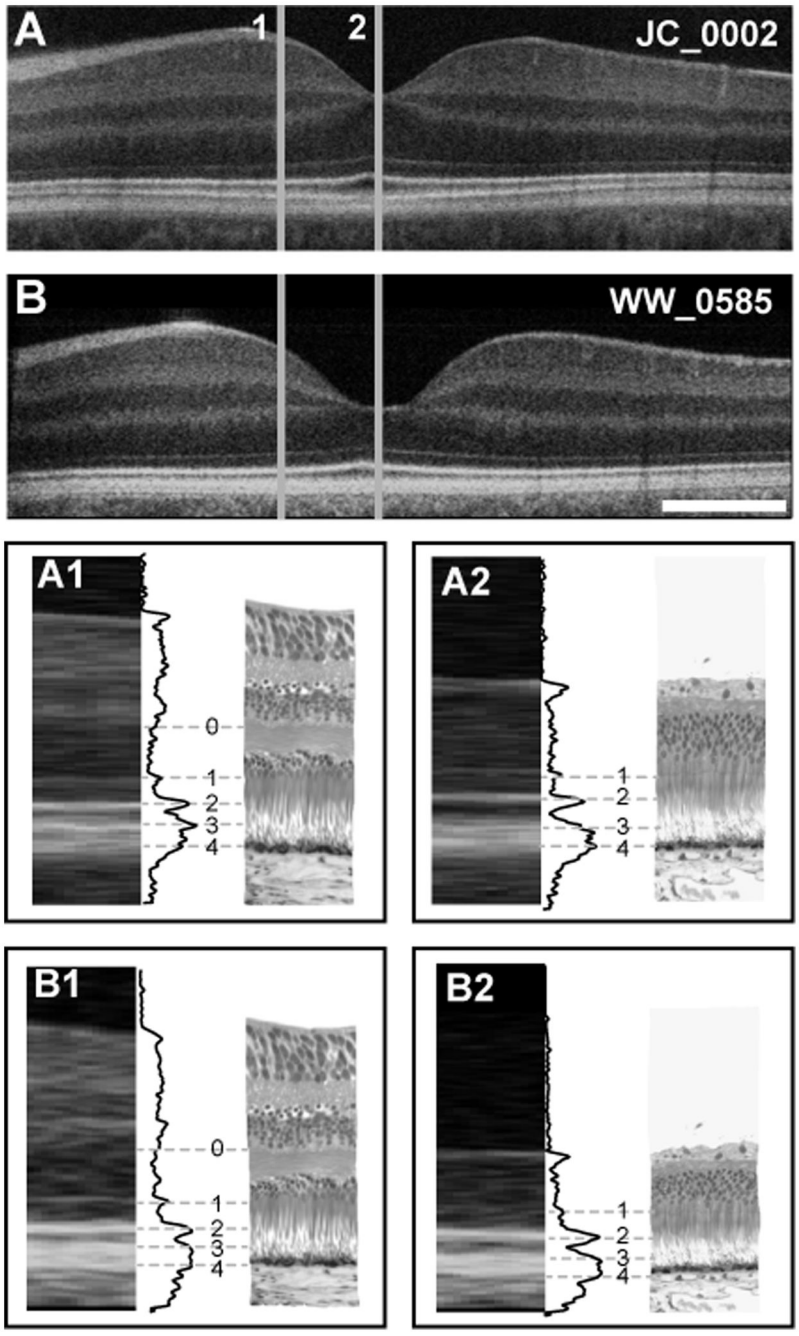

Figure 1.

Foveal layer assignment in the human retina. (A) Shown is an OCT image of a 28-year-old retina (JC_0002) and (B) a 17-month-old retina (WW_0585), compared to histology at parafoveal (1) and foveal (2) locations. A1 and B1 are the assignment of outer retinal layer bands 0–4, illustrated with grey lines connecting the OCT image, LRP and histological image for the parafoveal area. Band assignments in the foveal region are shown in A2 and B2. Scale bar is 500μm.

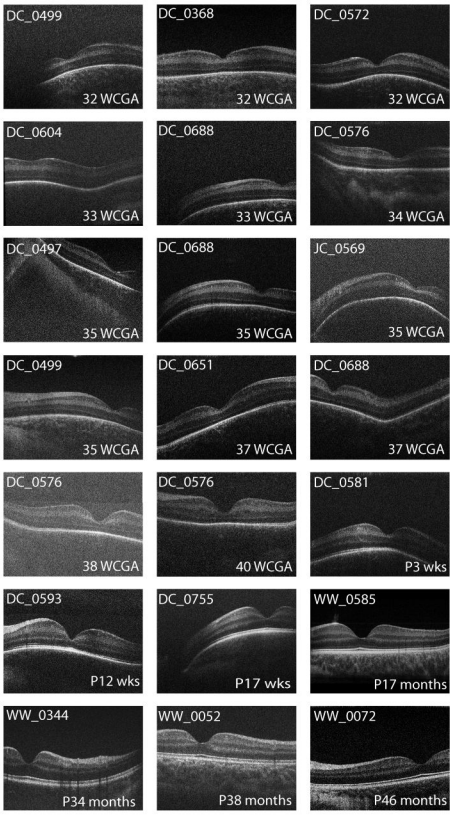

Figure 2.

Spectrum of foveal morphology observed with OCT. Shown are foveal scans from all exams meeting the inclusion criteria. Images are single frames extracted from a macular volume. Considerable variability exists at the 32 to 33 week PMA stage. By 17 months of age, the retina appears adult like. Another interesting feature is that some subjects have a dip like structure located temporally to the macula. We have termed this structure the “temporal divot”.

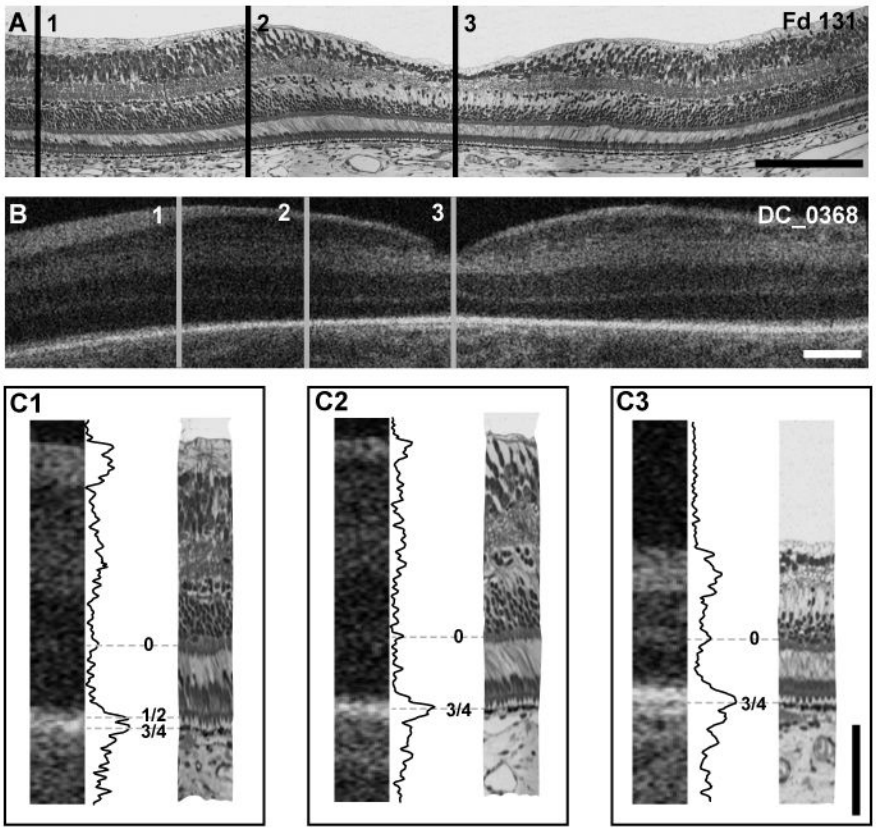

Figure 3.

Foveal development and layer assignment compared between a Fd 131 macaque (A) and 32 weeks PMA human infant (B, DC_0368). Lines 1 – 3 represent perifoveal, parafoveal and foveal locations, respectively. Insets C1–C3 at bottom are comparison of histology and OCT images, with layer assignment for perifoveal (C1), parafoveal (C2) and foveal (C3) locations. At the perifoveal location, bands 0, 1/2 and 3/4 are present, whereas only bands 0 and 3/4 are present at parafoveal and foveal locations. Scale bar in panels A & B is approximately 250 μm, horizontally; scale bar in panel C is 100 μm vertically.

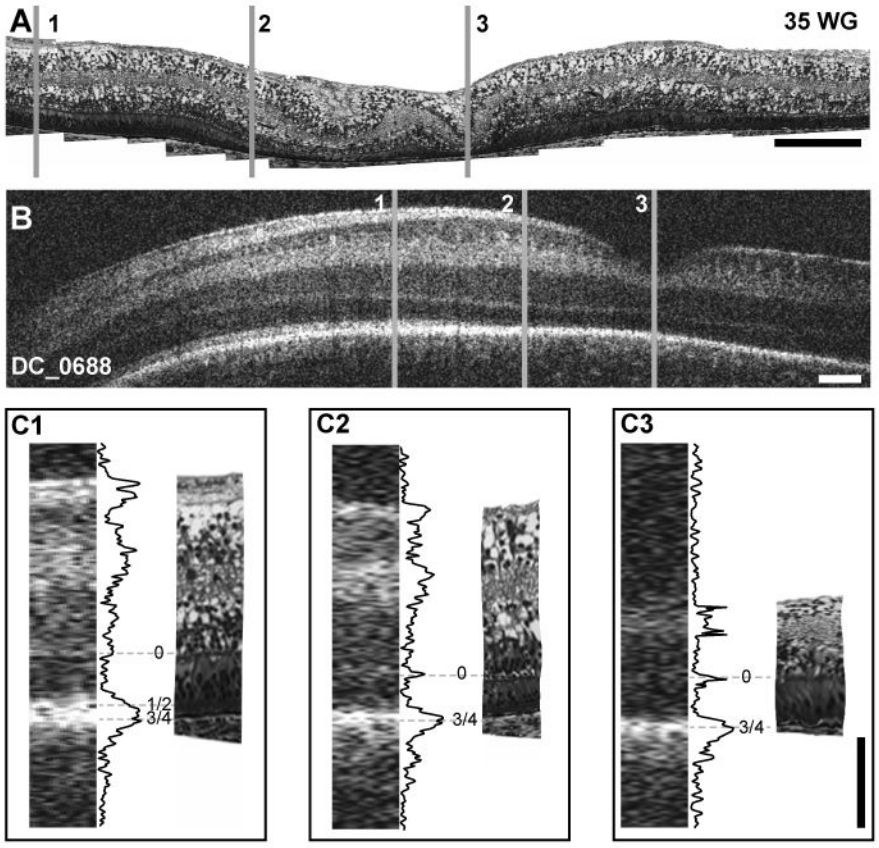

Figure 4.

Foveal development and layer assignment compared between 35 weeks PMA histological section from human donor (A) and 35 weeks PMA infant imaged with OCT (B- DC_0688). Lines 1 – 3 represent perifoveal, parafoveal and foveal locations, respectively. Insets C1–C3 at bottom are comparison of histology and OCT images, with layer assignment for perifoveal (C1), parafoveal (C2) and foveal (C3) locations. At the perifoveal location, bands 0, 1/2 and 3/4 are present, whereas only bands 0 and 3/4 are present at parafoveal and foveal locations. The 35 weeks PMA retina shows moderate edema in the central fovea, which causes buckling of the retina (between C2 and C3) and blister-like distortion of the innermost layer. Scale bar in panels A & B is approximately 250 μm, horizontally; scale bar in panel C is 100 μm vertically.

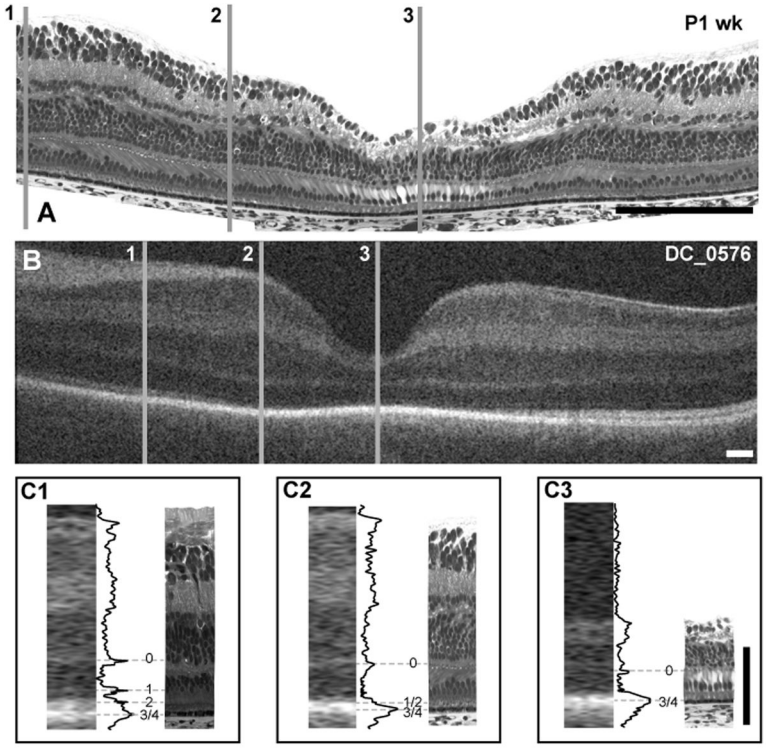

Figure 5.

Foveal development and layer assignment in a histological sample from a 41 weeks PMA human donor (A) and 38 weeks PMA infant (B-DC_0576). Gray lines 1 – 3 are representing perifoveal, parafoveal and foveola respectively. Insets C1–C3 at bottom are comparison of histology and OCT images, with layer assignment for perifoveal (C1), parafoveal (C2) and fovea (C3). At the perifoveal location, bands 0, 1, 2 and 3/4 are present, whereas only bands 0, 1/2 and 3/4 are present at parafoveal and band 0 and 3/4 at the fovea. Scale bar in panels A & B is approximately 250 μm, horizontally; scale bar in panel C is 100 μm vertically.

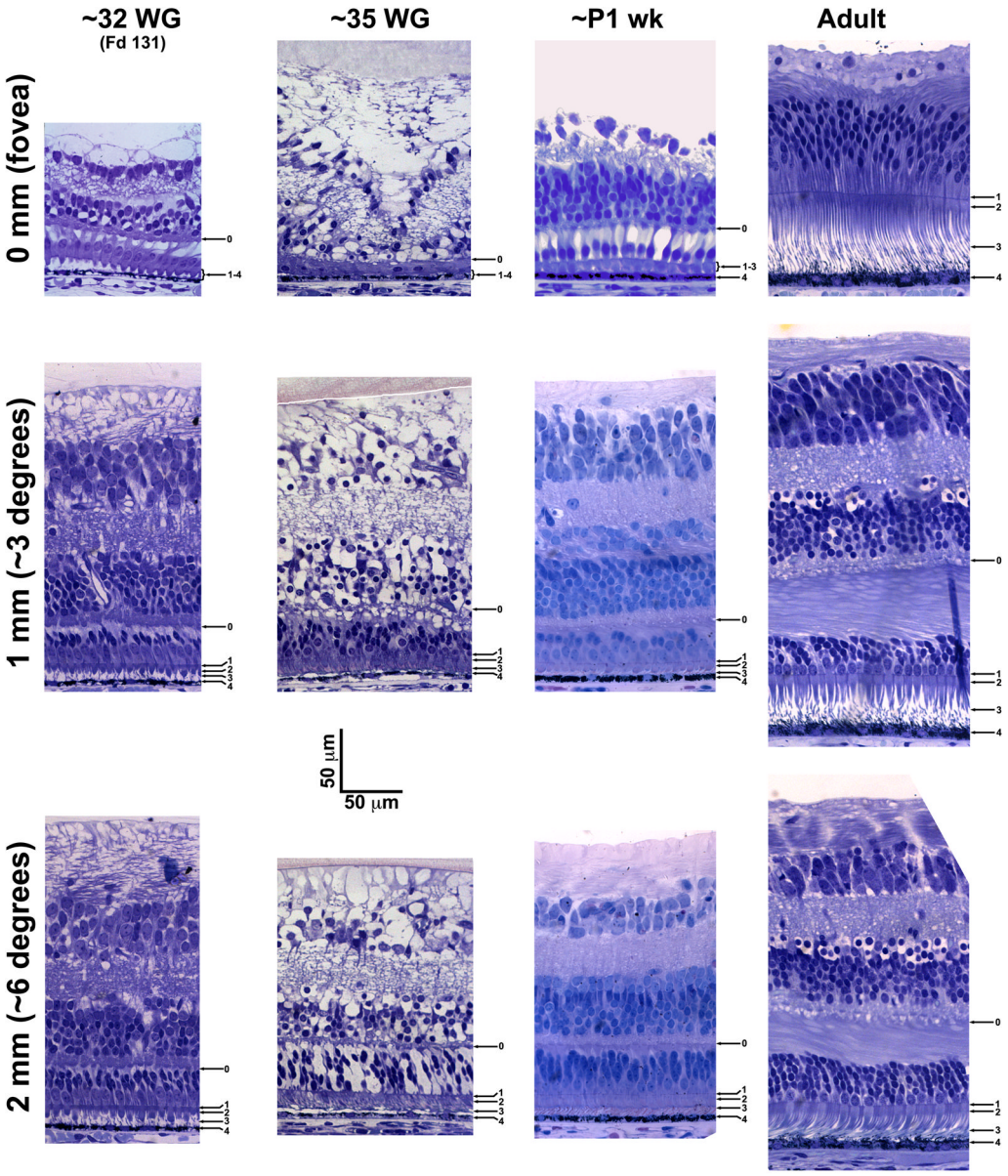

Figure 6.

Time course of photoreceptor maturation in fovea, parafoveal and perifoveal locations. Images are labeled with band assignments as seen in OCT. The 35 weeks PMA retina shows moderate edema in the central fovea, which causes buckling of the retina and blister-like distortion of the innermost layer, however these tissue artifacts do not interfere with layer identification. Arrows do not indicate layer thickness, simply the presence of a distinct band. Band 0 corresponds to the OPL, band 1 is the ELM, band 2 is the ISe, band 3 is the RPE/photoreceptor interdigitations and band 4 is the RPE. Images from the foveal (top row), parafoveal (middle row) and perifoveal (bottom row) region. Scale bar is 50 μm.

Table 1

	Eye Opening PCD (%CP)	Birth PCD (%CP)	FAZ Defined PCD (%CP)	Comparative Timepoint
Human	196 (100% CP) 28 weeks PMA	280 (143% CP) 40 weeks PMA	~180 (~90% CP) ~25–26 weeks PMA	32 weeks PMA = 224PCD *OR* 44 d (22% CP) after FAZ is defined
Macaque	123 (100% CP)	172 (138% CP)	~100–105 (~85% CP)	22% CP after FAZ defined is 105+27=133d

PCD – Post Conception Days

CP – Caecal Period